Frequency comb generation in non-centrosymmetric optical microresonators

Jan Szabados[a], Ingo Breunig[a,b], and Karsten Buse[a,b]

[a]Laboratory for Optical Systems, Department of Microsystems Engineering – IMTEK, University of Freiburg, Georges-Köhler-Allee 102, 79110 Freiburg, Germany
[b]Fraunhofer Institute for Physical Measurement Techniques IPM, Heidenhofstraße 8, 79110 Freiburg, Germany

ABSTRACT

Optical frequency combs are a key technology for precision measurements. In the past years, microresonator-based frequency combs based on third-order $\chi^{(3)}$ (Kerr) nonlinearities have attracted significant attention thanks to their small footprint and their wide-ranging applications in fields such as telecommunications, molecular spectroscopy or ultrafast distance measurements. In this contribution, we present a frequency comb generated in a microresonator made of 5% MgO-doped congruent lithium niobate, a non-centrosymmetric crystalline material, employing the generally much stronger second-order $\chi^{(2)}$-nonlinearities of such a material via a scheme of cascaded nonlinear processes. This approach paves the way towards reduced pump thresholds for comb generation and comes with intrinsic suitability for self-referencing.

Keywords: Nonlinear optics, Whispering gallery resonators, Microresonators, Frequency combs

1. INTRODUCTION

Optical frequency combs have shown to be of great use in a number of applications ranging from absolute optical precision spectroscopy in fundamental science,[1] ultrafast distance measurements (LIDAR),[2] dual-comb spectroscopy[3] and Tbit/s telecommunication[2] all the way to quantum signal and information processing.[4] The range of applications has seen dramatic growth especially since a frequency comb was first generated in an ultra-high-Q optical microresonator in 2007,[5] paving the way for miniaturized comb sources. The underlying processes for comb generation in this device relied on third-order $\chi^{(3)}$ (Kerr) nonlinearities, which have thus been the main focus of studies regarding microresonator-based frequency combs in recent years.[2,6–9] This type of frequency combs can only be generated around the pump wavelength and in the correct dispersion regime. For some applications such as astronomical spectrometer calibration[10] and f-$2f$-interferometry,[2] however, the initial comb needs to be transferred to shorter wavelengths. One obvious way of doing so is making use of second-order nonlinear-optical processes. Since many of the material platforms used for Kerr comb generation do not exhibit intrinsic $\chi^{(2)}$-nonlinearities, one straightforward solution is to use a separate cavity with such intrinsic $\chi^{(2)}$-nonlinearities, converting the frequency comb via second-harmonic and sum-frequency-generation.[11] An elegant approach to simplify this and to reduce the footprint of the setup is to use materials for Kerr-comb generation with intrinsic $\chi^{(2)}$-nonlinearities or to induce $\chi^{(2)}$-nonlinearities by e.g. electric fields,[12] stress through material growth[13] or ion migration.[14] This way, one can generate and convert a Kerr-comb in a single cavity as has been demonstrated for gallium phosphide,[15] aluminum nitride[10] and lithium niobate.[16] One can even use the electro-optic effect provided by the $\chi^{(2)}$-nonlinearity to generate the initial comb as has been demonstrated recently.[17,18] However, there is another elegant approach of generating frequency combs at both the pump and its second-harmonic simultaneously, stemming solely from $\chi^{(2)}$-nonlinearities. This approach is based on cascaded $\chi^{(2)}$-nonlinear-optical processes such as second-harmonic generation followed by optical parametric generation, again leading to second-harmonic and sum frequency generation and so on as visualized in Fig. 1a).[19] Here, combs are intrinsically generated around both the pump and second-harmonic frequencies, thus providing

Further author information: (Send correspondence to I.B.)
I.B.: E-mail: optsys@ipm.fraunhofer.de, Telephone: +49 761 203 97944.

in: Kudryashov, A.V.; Paxton, A.H.; Ilchenko, V.S.; Armani, A.M.; Society of Photo-Optical Instrumentation Engineers –SPIE: Laser Resonators, Microresonators, and Beam Control XXII. Proc. SPIE 11266, Paper 112660G (2020); doi: 10.1117/12.2544657

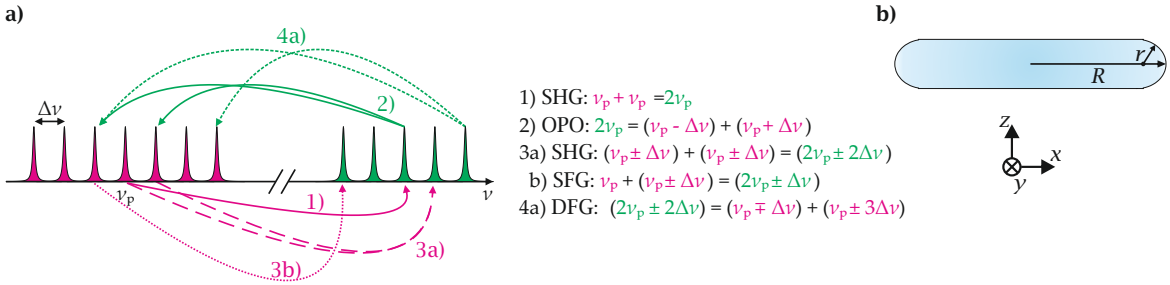

Figure 1. **a)** Second-order nonlinear-optical processes exploited to generate frequency combs around the pump frequency ν_p and the second-harmonic frequency $2\nu_p$. Abbreviations used: SHG: second-harmonic generation; OPO: optical parametric oscillation; SFG: sum frequency generation; DFG: difference frequency generation. **b)** Side view of the microresonator geometry. The geometry is characterized by the major radius $R = 1$ mm and the minor radius $r = 380$ µm.

intrinsic suitability for self-referencing. Additionally, as second-order nonlinearities are generally much stronger for continuous-wave light than third-order nonlinearities, this approach promises much lower pump thresholds. Although the idea has been around for more than 15 years, so far only a small number of experimental realizations is known, based either on large bow-tie cavities[20–24] or on relatively low-Q waveguide resonators,[25] and only very recently based on microresonators.[26,27] In this contribution, we present such a microresonator-enabled frequency comb based on cascaded $\chi^{(2)}$-nonlinearities.

2. METHODS

The microresonator is manufactured out of a 5%-MgO-doped z-cut congruent lithium niobate (CLN) crystal, since this material is easily available, inexpensive and has strong $\chi^{(2)}$-nonlinearities, making it one of the most widely employed materials for $\chi^{(2)}$-nonlinear optics.[28] We use a femtosecond laser source emitting at 388 nm wavelength with a 2 kHz repetition rate and 400 mW average output power to cut out a cylindrical preform of the crystal. This cylinder is subsequently glued to a metal post to allow for easier handling. Again using the femtosecond laser, we shape the resonator to end up with a geometry as shown in Fig. 1b) with a major radius of $R = 1$ mm and a minor radius of $r = 380$ µm. Then, to achieve optical-grade surface quality, we manually polish the resonator rim with diamond slurries.

As shown in Fig. 1a), to start the comb generation process, second-harmonic light has to be generated. In order for this to happen efficiently, one needs to make sure that the phase-matching criterion is fulfilled, meaning that the phase velocities $v_{\mathrm{ph,(p/sh)}} = c_0/n_{\mathrm{eff,(p/sh)}}$ for the pump and second-harmonic wavelengths need to match.[28] Here, c_0 is the vacuum speed of light, while $n_{\mathrm{eff,(p/sh)}}$ is the effective refractive index for the pump and second-harmonic waves, respectively, which can be determined numerically.[29,30] Phase-matching is fulfilled for temperatures around $T = 70$ °C when the resonator is pumped with ordinarily (o-) polarized light at 1064 nm, generating extraordinarily (e-) polarized light around 532 nm as shown in Fig. 2a).[31] This process is chosen for frequency comb generation. While the phase velocities match, however, the group velocities $v_{\mathrm{g,(p/sh)}} = 2\pi R \times \mathrm{FSR}_{\mathrm{(p,sh)}}$ of the two waves traveling around the resonator rim are offset by $\Delta\nu_g = 8 \times 10^6$ m/s. This is due to the different free spectral ranges (FSRs) of the two waves.

To characterize the microresonator and for the subsequent frequency comb generation, we built the experimental setup shown in Fig. 3. The resonator is pumped with ordinarily (o) polarized light from a fiber-coupled tunable laser source centered around 1064 nm as explained above. Once the power of the generated second-harmonic light exceeds the threshold for internally pumped OPO, sidebands are generated around the pump wavelength.[32] Eventually, after a sequence of further second-oder nonlinear-optical processes, combs build up around the pump as well as around the second-harmonic frequencies (Fig. 1a)). Due to the birefringent phase-matching we use, the comb around the pump will be o-polarized, whereas the comb around the second-harmonic frequency will be e-polarized. We can make use of this when designing our experimental setup: the rutile prism exhibits a large birefringence, thus separating the light around the pump and the second-harmonic frequencies spatially.

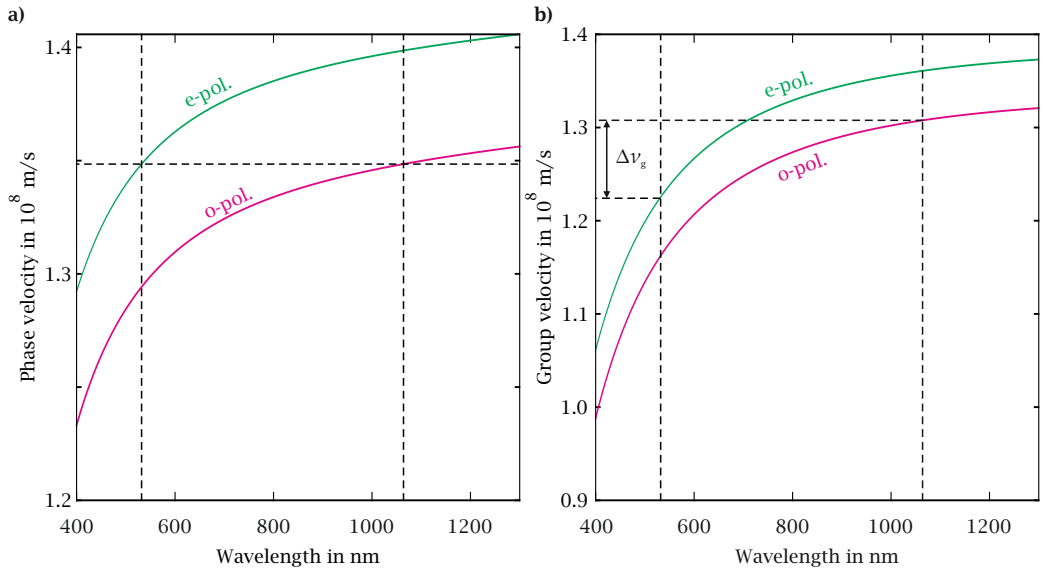

Figure 2. **a)** The phase velocities of the ordinarily (o) polarized light around the pump wavelength (pink curve) and the extraordinarily (e) polarized light around the second-harmonic wavelength (green curve) match for a temperature $T = 70$ °C, thus allowing for efficient second-harmonic generation. **b)** For the same situation, the group velocities of the pump and the second-harmonic light are offset by $\Delta\nu_g = 8 \times 10^6$ m/s.

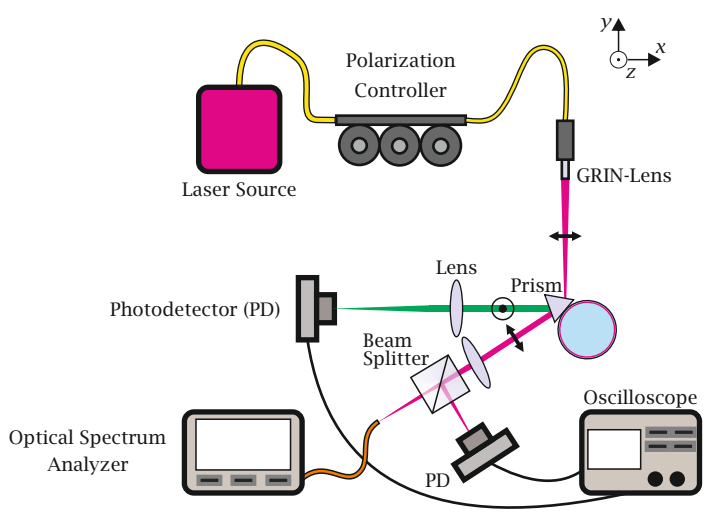

Figure 3. Setup used to acquire all experimental data presented in this contribution. Near-infrared light ($\lambda \approx 1064$ nm) from a fiber-coupled laser source (LS) with polarization controllers (PC) is focused through a gradient-index lens (GL) to couple light polarized in the x-y-plane to a microresonator by total internal reflection at the base of a rutile prism (P). When the resonator is heated to temperatures $T \approx 70$ °C, second-harmonic light is generated efficiently. Owing to the rather large birefringence of the prism, the outcoupled o-polarized light around the pump wavelength and the e-polarized light around the second-harmonic wavelength are separated spatially. The out-coupled light around the pump (plotted in pink) then passes a beam splitter (BS): a small portion of it is focused on a photodetector (PD) connected to an oscilloscope to observe the transmission spectrum of the resonator. A larger portion enters an optical spectrum analyzer (OSA) to observe the generated frequency spectrum. The light generated around the second-harmonic wavelength (plotted in green) is focused on another photodetector using a lens (L) to be able to optimize the second-harmonic generation efficiency.

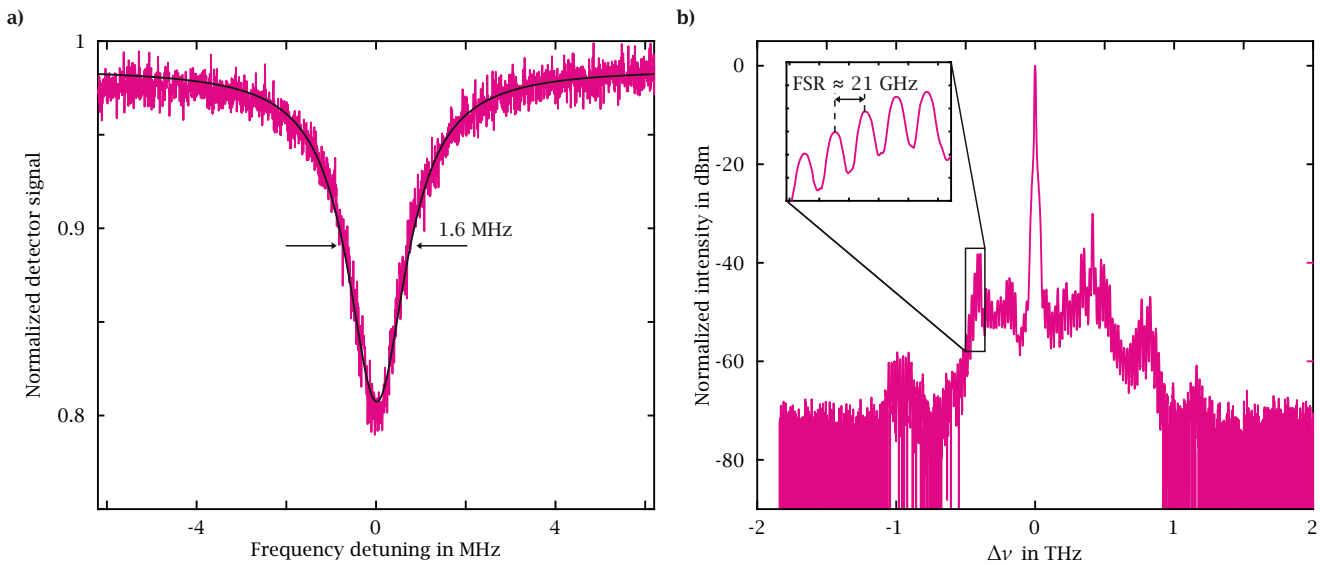

Figure 4. **a)** Transmission spectrum of the pump mode used for comb generation in critical coupling at input pump powers of a few µW. **b)** When the incoupled power is raised to the order of 2 mW, a frequency comb can be observed around the pump frequency. A close-up reveals the individual comb lines to be separated by about 21 GHz, corresponding to the free spectral range of the microresonator used at the pump frequency. The comb signal consists of approximately 100 individual lines.

3. RESULTS AND DISCUSSION

The microresonator is firstly characterized in critical coupling and at very low pump powers of a few µW. The resulting photodetector signal is shown in Fig. 4a). The full-width-at-half-maximum (FWHM) of the mode is 1.6 MHz, corresponding to $Q \approx 1.8 \times 10^8$.[28] From this measurement, one also obtains the maximum coupling efficiency to be $K_{\max} = 0.18$,[28] which is determined by imperfect spatial mode overlap of the incoupled laser light with the mode profile inside the resonator. In a next step, the pump power is ramped up to 10.3 mW. In critical coupling, we cannot observe cascaded second-order nonlinear-optical processes with the incoupled pump power being at its maximum of approximately $K_{\max} \times 10.3$ mW ≈ 1.9 mW. Thus, we increase the distance between the resonator and the prism slightly, hence entering the undercoupling regime. This leads to an increase of the quality factor Q and a decrease of the incoupled pump power.[28] In this regime, we can observe a roughly 2-THz-broad comb signal in the near-infrared with the optical spectrum analyzer used. Since the individual comb-lines are separated by approximately 21 GHz, corresponding to the free spectral range of the microresonator at the pump wavelength, the obtained comb consists of about 100 individual comb lines. This result points towards a modulation-instability-induced frequency comb since very similar spectra were observed for a frequency comb based on second-order-nonlinearities in a bulky bow-tie cavity recently.[24] The modulation-instability-gain has also been determined numerically in one of our own contributions.[26]

4. OUTLOOK AND CONCLUSION

The span of the frequency comb demonstrated here is most probably limited as the group velocity difference between the pump and second-harmonic waves of $\Delta\nu_{\mathrm{g}} = 8 \times 10^6$ m/s (Fig. 2b)) leads to the two waves traveling around the resonator rim showing reduced temporal overlap. This leads to a reduction of the available interaction length and thus limits the span of the generated combs as well as the generation efficiency, i.e. the pump threshold. One way to overcome this would be to choose better-suited wavelength regimes with a reduced FSR-offset for comb generation and to account for the phase-mismatch by employing a so-called quasi-phase-matching (QPM) structure as has been demonstrated for this type of resonators earlier.[28] Using a QPM-structure would furthermore allow to choose the center wavelengths of the generated combs almost arbitrarily within the transmission window of the material platform employed. While this proof-of-principle device still leaves a lot of room for improvement, this new way of generating frequency combs comes with the major advantage of using

the generally stronger $\chi^{(2)}$-nonlinearities instead of the $\chi^{(3)}$-nonlinearities used in microresonator-based combs so far. We already observe combs at pump thresholds of the order of 2 mW: for Kerr-combs, which have been around since 2007, highly-optimized systems exhibit today thresholds of slightly below 1 mW, while in microresonators of a similar size to the one used here, minimum thresholds of around 3 mW are found.[33] Because of this, this proof-of-principle device might lead to significant research activities. Furthermore, the scheme implemented for comb generation here can obviously be applied to any material exhibiting second-order nonlinearities. One could for example think of accessing highly challenging wavelength regimes such as the mid-infrared using non-oxide materials such as $AgGaSe_2$ or $CdSiP_2$, for which the crucial initial step of optical parametric oscillation in a microresonator has already been demonstrated.[34,35] Also, while we rely on hand-polished, individually manufactured microresonators in this contribution, the method introduced here could also be extended to batch-compatible chip-integrated microresonators. Recently, optical parametric oscillation was demonstrated for the first time on such a platform, potentially paving the way for chip-integrated frequency comb sources.[36] This would increase the scalability of the platform introduced here, making it more appealing for applications. The results presented in this contribution can be considered a first step towards uncovering the full potential of microresonator frequency combs based on cascaded $\chi^{(2)}$-nonlinear-optical processes.

ACKNOWLEDGMENTS

Funding: Fraunhofer and Max Planck Cooperation Program (COSPA).

REFERENCES

[1] Diddams, S. A., Udem, T., Bergquist, J. C., Curtis, E. A., Drullinger, R. E., Hollberg, L., Itano, W. M., Lee, W. D., Oates, C. W., Vogel, K. R., and Wineland, D. J., "An optical clock based on a single trapped $^{199}Hg^+$ ion," *Science* **293**, 825–828 (2001).

[2] Gaeta, A. L., Lipson, M., and Kippenberg, T. J., "Photonic-chip-based frequency combs," *Nat. Photon.* **13**, 158–169 (2019).

[3] Picqué, N. and Hänsch, T. W., "Frequency comb spectroscopy," *Nat. Photon.* **13**, 146–157 (2019).

[4] Kues, M., Reimer, C., Lukens, J. M., Munro, W. J., Weiner, A. M., Moss, D. J., and Morandotti, R., "Quantum optical microcombs," *Nat. Photon.* **13**, 170–179 (2019).

[5] Del'Haye, P., Schliesser, A., Arcizet, O., Wilken, T., Holzwarth, R., and Kippenberg, T. J., "Optical frequency comb generation from a monolithic microresonator," *Nature* **450**, 1214–1217 (2007).

[6] Chembo, Y. K., Strekalov, D. V., and Yu, N., "Spectrum and dynamics of optical frequency combs generated with monolithic whispering gallery mode resonators," *Phys. Rev. Lett.* **104**, 103902 (2010).

[7] Kippenberg, T. J., Holzwarth, R., and Diddams, S. A., "Microresonator-based optical frequency combs," *Science* **332**, 555–559 (2011).

[8] Hansson, T., Modotto, D., and Wabnitz, S., "Dynamics of the modulational instability in microresonator frequency combs," *Phys. Rev. A* **88**, 023819 (2013).

[9] Kippenberg, T. J., Gaeta, A. L., Lipson, M., and Gorodetsky, M. L., "Dissipative Kerr solitons in optical microresonators," *Science* **361**, eaan8083 (2018).

[10] Guo, X., Zou, C.-L., Jung, H., Gong, Z., Bruch, A., Jiang, L., and Tang, H. X., "Efficient generation of a near-visible frequency comb via Cherenkov-like radiation from a Kerr microcomb," *Phys. Rev. Appl.* **10**, 014012 (2018).

[11] Herr, S. J., Brasch, V., Szabados, J., Obrzud, E., Jia, Y., Lecomte, S., Buse, K., Breunig, I., and Herr, T., "Frequency comb up- and down-conversion in synchronously driven $\chi^{(2)}$ optical microresonators," *Opt. Lett.* **43**, 5745–5748 (2018).

[12] Timurdogan, E., Poulton, C. V., Byrd, M. J., and Watts, M. R., "Electric field-induced second-order nonlinear optical effects in silicon waveguides," *Nat. Photon.* **11**, 200–206 (2017).

[13] Levy, J. S., Foster, M. A., Gaeta, A. L., and Lipson, M., "Harmonic generation in silicon nitride ring resonators," *Opt. Express* **19**, 11415–11421 (2011).

[14] Billat, A., Grassani, D., Pfeiffer, M. H. P., Kharitonov, S., Kippenberg, T. J., and Brès, C.-S., "Large second harmonic generation enhancement in Si_3N_4 waveguides by all-optically induced quasi-phase-matching," *Nat. Commun.* **8**, 1016 (2017).

[15] Wilson, D. J., Schneider, K., Hönl, S., Anderson, M., Kippenberg, T. J., and Seidler, P., "Integrated gallium phosphide nonlinear photonics," *ArXiv e-prints* , 1808.03554 (2018).
[16] He, Y., Yang, Q.-F., Ling, J., Luo, R., Liang, H., Li, M., Shen, B., Wang, H., Vahala, K., and Lin, Q., "Self-starting bi-chromatic $LiNbO_3$ soliton microcomb," *Optica* **6**, 1138–1144 (2019).
[17] Rueda, A., Sedlmeir, F., Kumari, M., Leuchs, G., and Schwefel, H. G. L., "Resonant electro-optic frequency comb," *Nature* **568**, 378–381 (2019).
[18] Zhang, M., Buscaino, B., Wang, C., Shams-Ansari, A., Reimer, C., Zhu, R., Kahn, J. M., and Lončar, M., "Broadband electro-optic frequency comb generation in a lithium niobate microring resonator," *Nature* **568**, 373–377 (2019).
[19] Buryak, A. V., Di Trapani, P., Skryabin, D. V., and Trillo, S., "Optical solitons due to quadratic nonlinearities: from basic physics to futuristic applications," *Phys. Rep.* **370**, 63–235 (2002).
[20] Ulvila, V., Phillips, C. R., Halonen, L., and Vainio, M., "Frequency comb generation by a continuous-wave-pumped optical parametric oscillator based on cascading quadratic nonlinearities," *Opt. Lett.* **38**, 4281–4284 (2013).
[21] Ulvila, V., Phillips, C. R., Halonen, L., and Vainio, M., "High-power mid-infrared frequency comb from a continuous-wave-pumped bulk optical parametric oscillator," *Opt. Express* **22**, 10535–10543 (2014).
[22] Ricciardi, I., Mosca, S., Parisi, M., Maddaloni, P., Santamaria, L., De Natale, P., and De Rosa, M., "Frequency comb generation in quadratic nonlinear media," *Phys. Rev. A* **91**, 063839 (2015).
[23] Mosca, S., Ricciardi, I., Parisi, M., Maddaloni, P., Santamaria, L., De Natale, P., and De Rosa, M., "Direct generation of optical frequency combs in $\chi^{(2)}$ nonlinear cavities," *Nanophotonics* **5**, 316–331 (2016).
[24] Mosca, S., Parisi, M., Ricciardi, I., Leo, F., Hansson, T., Erkintalo, M., Maddaloni, P., De Natale, P., Wabnitz, S., and De Rosa, M., "Modulation instability induced frequency comb generation in a continuously pumped optical parametric oscillator," *Phys. Rev. Lett.* **121**, 093903 (2018).
[25] Ikuta, R., Asano, M., Tani, R., Yamamoto, T., and Imoto, N., "Frequency comb generation in a quadratic nonlinear waveguide resonator," *Opt. Express* **26**, 15551–15558 (2018).
[26] Szabados, J., Puzyrev, D. N., Minet, Y., Reis, L., Buse, K., Villois, A., Skryabin, D. V., and Breunig, I., "Frequency comb generation via cascaded second-order nonlinearities in microresonators," *ArXiv e-prints* , 1912.00945 (2019).
[27] Hendry, I., Trainor, L. S., Xu, Y., Coen, S., Murdoch, S. G., Schwefel, H. G. L., and Erkintalo, M., "Experimental observation of internally-pumped parametric oscillation and quadratic comb generation in a $\chi^{(2)}$ whispering-gallery-mode microresonator," *ArXiv e-prints* , 1912.02804 (2019).
[28] Breunig, I., "Three-wave mixing in whispering gallery resonators," *Laser Photonics Rev.* **10**, 569–587 (2016).
[29] Gorodetsky, M. L. and Fomin, A. E., "Geometrical theory of whispering-gallery modes," *IEEE J. Sel. Top. Quantum Electron.* **12**, 33–39 (2006).
[30] Umemura, N., Matsuda, D., Mizuno, T., and Kato, K., "Sellmeier and thermo-optic dispersion formulas for the extraordinary ray of 5 mol. % MgO-doped congruent $LiNbO_3$ in the visible, infrared, and terahertz regions," *Appl. Opt.* **53**, 5726–5732 (2014).
[31] Fürst, J. U., Strekalov, D. V., Elser, D., Lassen, M., Andersen, U. L., Marquardt, C., and Leuchs, G., "Naturally phase-matched second-harmonic generation in a whispering-gallery-mode resonator," *Phys. Rev. Lett.* **104**, 153901 (2010).
[32] Hansson, T., Leo, F., Erkintalo, M., Anthony, J., Coen, S., Ricciardi, I., De Rosa, M., and Wabnitz, S., "Single envelope equation modeling of multi-octave comb arrays in microresonators with quadratic and cubic nonlinearities," *J. Opt. Soc. Am. B* **33**, 1207–1215 (2016).
[33] Zhang, S., Silver, J. M., Del Bino, L., Copie, F., Woodley, M. T. M., Ghalanos, G. N., Svela, A. Ø., Moroney, N., and Del'Haye, P., "Sub-milliwatt-level microresonator solitons with extended access range using an auxiliary laser," *Optica* **6**, 206–212 (2019).
[34] Meisenheimer, S.-K., Fürst, J. U., Buse, K., and Breunig, I., "Continuous-wave optical parametric oscillation tunable up to an 8 µm wavelength," *Optica* **4**, 189–192 (2017).
[35] Jia, Y., Hanka, K., Zawilski, K. T., Schunemann, P. G., Buse, K., and Breunig, I., "Continuous-wave whispering-gallery optical parametric oscillator based on $CdSiP_2$," *Opt. Express* **26**, 10833–10841 (2018).
[36] Bruch, A. W., Liu, X., Surya, J. B., Zou, C. L., and Tang, H. X., "On-chip $\chi^{(2)}$ microring optical parametric oscillator," *Optica* **6**, 1361–1366 (2019).